[CANCER RESEARCH 63, 5084–5090, August 15, 2003]

Targeted Actinium-225 *in Vivo* Generators for Therapy of Ovarian Cancer[1]

Paul E. Borchardt, Rui R. Yuan, Matthias Miederer, Michael R. McDevitt, and David A. Scheinberg[2]

Department of Molecular Pharmacology and Chemistry, Memorial Sloan-Kettering Cancer Center, New York, New York 10021

ABSTRACT

Advanced ovarian cancer is largely incurable, but initially it is frequently confined to the i.p. space. We explored i.p. radioimmunotherapy in a mouse model of human ovarian cancer. Use of a targeted actinium-225 (^{225}Ac) *in vivo* generator of α particles exploits the extreme, selective cytotoxicity of α particles, while providing a feasible half-life to enable delivery to tumor. ^{225}Ac chelated with 2-(*p*-isothiocyanatobenzyl)-1,4,7,10-tetraazacyclododecane-1,4,7,10 tetraacetic acid was conjugated to trastuzumab, an anti-HER-2/*neu* antibody. The radioimmunoconjugate was tested for immunoreactivity, internalization, and cytotoxicity using a human ovarian carcinoma cell line, SKOV3. ^{225}Ac-labeled trastuzumab retained immunoreactivity (50–90%), rapidly internalized into cells (50% at 2 h), and had an ED_{50} of 1.3 nCi/ml after 4 days of incubation *in vitro*. i.p. administered ^{225}Ac- or ^{111}In-labeled trastuzumab behaved similarly with high tumor uptake [56–60% injected dose per gram (% ID/g) at 4 h, which increased to 65–70% ID/g at 24 h]. Tumor uptake was 3–5-fold higher than liver and spleen, the normal organs with the highest uptake. i.v. administration of ^{111}In-labeled trastuzumab produced slightly higher normal organ uptake compared with i.p.-administered ^{111}In-labeled trastuzumab. However, tumor uptake was low, 5%–26% ID/g. Therapy was examined with native trastuzumab and 220, 330, and 450 nCi of ^{225}Ac-labeled trastuzumab or ^{225}Ac-labeled control antibody at different dosing schedules. Therapy was initiated 9 days after tumor seeding. Groups of control mice and those administered native trastuzumab had median survivals of 33 and 37 or 44 days, respectively. Median survival was 52–126 days with ^{225}Ac-labeled trastuzumab at various doses and schedules, and 48–64 days for ^{225}Ac-labeled control the same schedules. Deaths from toxicity occurred with the highest activity levels. In conclusion, i.p. administration with a ^{225}Ac-labeled internalizing anti-HER-2/*neu* antibody can extend survival significantly in a nude mouse model of human ovarian cancer at levels that produce no apparent gross toxicity.

INTRODUCTION

α particle emitting radioisotopes are attractive for RIT[3] of micrometastases because of the extreme cytotoxicity and short path length (40–80 μm, roughly 2–5 cell diameters) of the α particles. Cell death may result from as few as one α particle traversal through the nucleus (1). The much shorter average path length of α compared with β particles (average ranges, 0.8–5 mm) largely eliminates nonspecific irradiation to surrounding tissue (2). However, these attributes are countered by the short half-lives of the best studied radioisotopes, which include astatine-211 (^{211}At), $T_{1/2}$ = 7 h, bismuth-212 (^{212}Bi), $T_{1/2}$ = 60 min, and bismuth-213 (^{213}Bi), $T_{1/2}$ = 46 min (3). The short half-lives prohibit the synthesis of radioimmunoconjugates from these isotopes at a central radiopharmacy distant from the patient and reduce their applicability for i.v.-administered RIT of bulky solid tumors, where peak tumor uptake is usually delayed for hours to days after administration.

To overcome the limitations imposed by the short half-lives of the isotopes we developed an *in vivo* generator of α particles based on the α emitter actinium-225 (^{225}Ac), which has a 10-day half-life (4). It is a parent in a decay cascade that produces three additional α particle emitting radioisotopes including ^{213}Bi. (Fig. 1; Ref. 5). The resultant *in vivo* generator system has an ED_{50} on cellular proliferation in the range of 8–2000 pCi/ml and produces long-term remissions and cures in mouse models of disseminated lymphoma and localized prostate carcinoma (4).

Late-stage ovarian cancer is often characterized by metastatic seeding of the peritoneal surface and accounts for 75–85% of all of the newly diagnosed ovarian cancer patients (6). Standard therapy for patients with peritoneal implants is cytoreductive surgery and combination chemotherapy, which produces up to a 50% complete response rate (7); half of these patients later relapse with chemoresistant disease and are not adequately rescued by additional therapy (6, 7).

The regional localization of ovarian cancer prompted the development of i.p. RIT with β emitting radioisotopes (8–13). The administration of radiolabeled antibody into the tumor compartment provides direct access to tumor antigen with higher initial antibody concentrations that favor tumor binding. Moreover, the slow egress of radiolabeled antibody from the peritoneal cavity to the circulatory system reduces peak and accumulative blood radioactivity compared with i.v. administration (10, 12). Higher activities can be administered with i.p. RIT before the induction of myelotoxicity, the dose-limiting toxicity (10, 12). Clinical studies demonstrate some therapeutic advantages for i.p. administration in an adjuvant setting and in the treatment of minimal residual disease, but the results with bulky disease are disappointing (8, 9, 13).

In this study, we have now tested a ^{225}Ac-based *in vivo* generator in a mouse model of advanced ovarian cancer. We found that ^{225}Ac-labeled immunoconjugates can treat regional disease in this model and, therefore, provide an expanded possible use of the *in vivo* generator technology (4). These studies seek to expand the possible use of *in vivo* generators beyond our previous examples (4).

MATERIALS AND METHODS

Monoclonal Antibodies. Trastuzumab (Herceptin; Genentech, South San Francisco, CA) is a humanized IgG1 that recognizes the extracellular domain of the HER-2/*neu* oncoprotein (14). The antibody was washed with 0.1 M PBS (pH 7.3) before labeling using a centrifugal concentrator (Centriplus; Millipore, Bedford, MA) to remove formulating agents.

HuM195 (Protein Design Labs, Fremont, CA) is a humanized IgG1 that recognizes an extracellular domain on CD33 and served as an isotype-matched nonspecific antibody control (15).

Cell Line. The human epithelial ovarian carcinoma cell line SKOV3-NMP2 was derived from serial passage of the parental SKOV3 cell line in nude mice (16). It was grown in McCoy's 5A medium supplemented with 1.5 g/liter $NaHCO_3$, 10% fetal bovine serum, nonessential amino acids, and penicillin (10 units/ml)/streptomycin (10 μg/ml) at 37°C in 5% CO_2. Cells were detached with 0.25% trypsin/0.1% EDTA in PBS.

Preparation of Radioimmunoconjugates. Briefly, a two-step radiolabeling protocol was used where the radiometals, ^{225}Ac and ^{111}In, were first chelated with 2-(*p*-isothiocyanatobenzyl)-1,4,7,10-tetraazacyclododecane-1,4,7,10 tetraacetic acid and then conjugated to an antibody. After column purification, the radioimmunoconjugates were quality controlled before use (17). The two-step protocol was developed to overcome the very low radiolabeling efficiency, <1%, and poor *in vitro* stability that results from radio-

Received 9/18/02; revised 5/27/03; accepted 6/6/03.

The costs of publication of this article were defrayed in part by the payment of page charges. This article must therefore be hereby marked *advertisement* in accordance with 18 U.S.C. Section 1734 solely to indicate this fact.

[1] Supported in part by Grant R01-CA55349 and The Doris Duke Charitable Trust.

[2] To whom requests for reprints should be addressed, at Department of Molecular Pharmacology and Chemistry, Memorial Sloan-Kettering Cancer Center, New York, NY 10021. E-mail: d-scheinberg@ski.mskcc.org.

[3] The abbreviations used are: RIT, radioimmunotherapy; HSA, human serum albumin; $T_{1/2}$, half-time; % ID/g, % of injected dose/g.

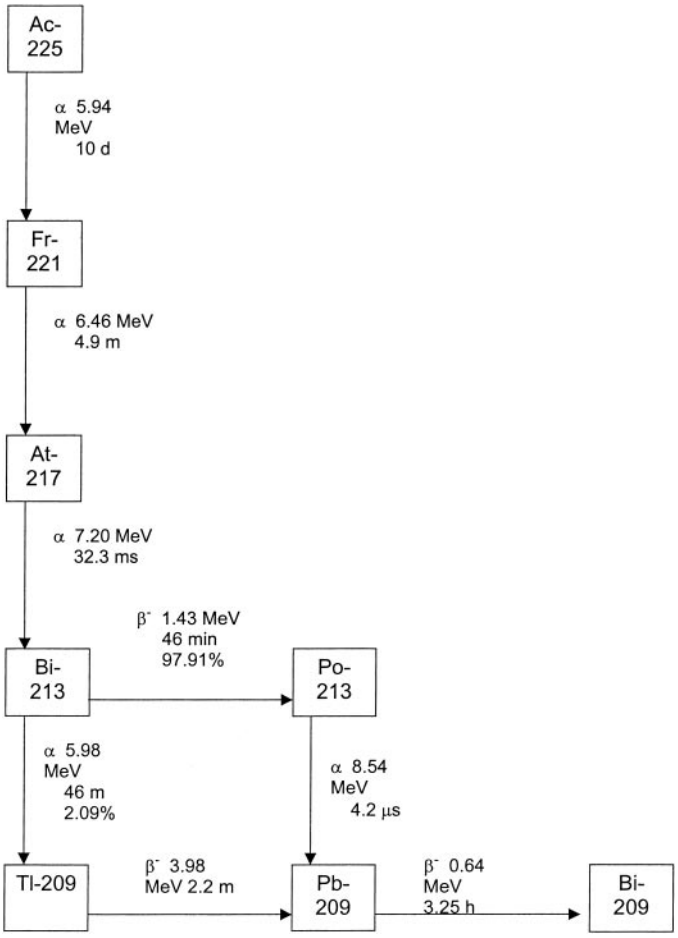

Fig. 1. ^{225}Ac decay cascade with particulate emissions, half-lives, and abundance. Transformations with <0.1% occurrence omitted.

labeling a DOTA-derived immunoconjugate with ^{225}Ac using a conventional one-step methodology (4).

Either $^{225}AcNO_3$ (Oak Ridge National Labs, Oak Ridge, TN) dissolved in 0.1 M HCl or ^{111}InCl (NEN Life Science Products, Inc., Boston, MA) was added to 10 μl of 2-(*p*-isothiocyanatobenzyl)-1,4,7,10-tetraazacyclododecane-1,4,7,10 tetraacetic acid, 10 mg/ml (Macrocyclics, Richardson, TX). Typically, 0.5–1 mCi of ^{225}Ac, 8–100 μl, or 0.5–1 mCi ^{111}In, 1–5 μl, was used with the activity of the ^{225}Ac determined using a drop well dose calibrator (CRC-17; E.R. Squibb and Sons, Inc., Princeton, NJ) set at 775 and the reading multiplied by 5. After the addition of the radiometal to the chelate, the pH of the solution was raised to 4.5–5.5 with the addition of 10–75 μl of 1 M tetramethyl ammonium acetate (Aldrich Chemical Co., Milwaukee, WI). Ascorbic acid, 5 μl, 150 g/liter, was added as a radioprotectant, and the pH checked again and adjusted if necessary with additional 1 M tetramethyl ammonium acetate. The solution was incubated at 56°C for 1 h.

The percentage of incorporation of the radiometal by the chelate was determined by loading 0.5–1 μl of the solution onto a 1-ml cation exchange resin (Sephadex C-25; Amersham Pharmacia Biotech Inc., Piscataway, NJ) equilibrated with 0.9% saline and eluting the column with 3 ml of saline. The eluate was collected, and the activity of the eluate and the column measured immediately and then again the next day in case of ^{225}Ac, using a Na-I detector (Canberra Industries, Meriden, CT). Chelated radiometals elute, whereas the free radiometals are retained on the column. To label the antibodies, the chelated radiometal was then added to 200 μg of antibody, 16–204 μl, and the pH raised to 8.0–9.0 with the addition of 10–40 μl of 1 M $NaHCO_2/Na_2CO_2$ buffer (pH 9.5). The solution was incubated for 30 min at 36°C. To complex any loosely bound radiometal before purification 10–40 μl of 10 mM EDTA was added and the solution incubated for 5–10 min.

The radioimmunoconjugate was loaded onto a 10-ml size exclusion column (10DG; Bio-Rad, Hercules, CA) that was equilibrated previously with 1% HSA in saline. The radioimmunoconjugate was eluted with 1% HSA, and 1 ml fractions were collected and assayed for activity using a drop well dose calibrator. The measured activities of ^{225}Ac are initially inaccurate because of the retention of ^{225}Ac daughter radioisotopes on the column and disruption of the secular equilibrium. This does not impede running the quality control tests but requires that accurate dosing of the drugs and measuring the activity of assay samples wait until secular equilibrium is achieved, ~5 h.

The radiochemical purity of the radioimmunoconjugates was determined by instant TLC (SG ITLC plates; Gelman Science Inc., Ann Arbor, MI; Ref. 18). The strips were analyzed immediately in the case of ^{111}In or allowed to sit overnight for ^{225}Ac. Analysis was performed using a gas ionization detector (Ambis 4000; Ambis, San Diego, CA).

The immunoreactivity of the purified, radiolabeled trastuzumab was determined by incubating the radiolabeled trastuzumab with SKOV3-NMP2 cells. First, cells were washed twice with ice-cold PBS and then blocked by incubation on ice with 2% rabbit serum. Then 5 ng of the radiolabeled antibody in 1–3 μl of 1% HSA was added to 10^7 cells, and the cell pellets incubated on ice for 30 min. The cells were washed twice with ice-cold PBS, and the washes were saved and counted by scintigraphy along with the cells after 20-h time elapsed.

Internalization Study. Harvested SKOV3-NMP2 cells were washed twice with ice-cold PBS and then incubated on ice with 2% rabbit serum for 20 min. After a wash with ice-cold PBS the cells were resuspended in medium at a density of 10^7 cells/ml. Trastuzumab radiolabeled with ^{225}Ac, 10 ng/ml, was added, and two 400 μl samples were immediately taken and processed as described below. The cells were then placed in a humidified, 37°C incubator with 5% CO_2 where they were periodically swirled and sampled at 0.5, 1, 2, and 4 h. The cells were centrifuged, washed twice with 1 ml of ice-cold PBS, and then 1 ml of an acidic stripping buffer [50 mM glycine/150 mM NaCl (pH 2.8)] was added. The cells were incubated for 10 min at room temperature, centrifuged, and the supernatant removed and saved for counting. The pellet was then transferred to a separate scintillation vial for counting. The vials were counted the following day, and the percentages of membrane-bound (acid-strippable) and internalized counts were then determined.

***In Vitro* Cell Cytotoxicity.** SKOV3-NMP2 cells were washed twice with PBS and seeded into 96-well flat-bottomed plates at a density of 2.5×10^3 cells in 100 μl of medium. Serial dilutions of ^{225}Ac-labeled trastuzumab were made using a starting activity concentration of 10 nCi/ml and a specific activity of 0.4 μCi/μg. One-hundred μl of the ^{225}Ac-labeled trastuzumab was added to half of the wells, whereas the other half received 100 μl of the ^{225}Ac-labeled trastuzumab supplemented with native trastuzumab at a concentration of 5×10^{-7} M to block binding of the radiolabeled antibody. The 96-well plates were placed into a humidified 37°C incubator with 5% CO_2. After 3, 4, or 5 days of incubation, cell viability was determined by tritiated thymidine incorporation (Perkin-Elmer Life Sciences, Boston, MA). Cells that received no antibody or unlabeled antibody served as controls.

Mouse Model. Female athymic nude mice, 4–8 weeks of age (Taconic, Germantown, NY) were inoculated i.p. with 5×10^6 SKOV3-NMP2 cells in a volume of 500 μl of medium. For the biodistribution experiments, mice were treated with radioimmunoconjugate 19 days after inoculation. For the therapy experiments, mice were treated 9 days after inoculation.

Mice were housed in filter-top cages and provided with sterile food, water, and bedding. Animal protocols were approved by the Animal Care and Use Committee at Memorial Sloan-Kettering Cancer Center.

Radioimmunoconjugate Administration to Nude Mice. The radioimmunoconjugates were diluted with 1% HSA in saline to the appropriate activities. For i.p. administration, mice were first anesthetized with an i.m. injection of 30 μl of a 4.3:1 ratio of ketamine, 100 mg/ml: xylazine, 20 mg/ml. After administration of the radioimmunoconjugate the mice were placed on their backs. Mice that received i.v. administration received the same quantity of anesthesia by i.p. administration after dilution to 500 μl in saline. Injection volumes were 200 μl for i.p. administration and 150 μl for i.v. administration via the retro-orbital route. The syringes were weighed before and after injection to determine the administered activity.

Biodistributions. Mice were administered i.p. ^{225}Ac-labeled trastuzumab, ^{111}In-labeled trastuzumab, or ^{111}In-labeled HuM195, or received i.v. ^{111}In-labeled trastuzumab. Groups of mice were sacrificed at 1, 4, 24, 48, and 120 h after administration by CO_2 asphyxiation except for mice that received i.v. ^{111}In-labeled trastuzumab. These were sacrificed at 4 and 24 h after adminis-

tration. Blood, tumor, and the major organs: heart, lung, stomach, intestine, spleen, muscle, bone, liver, and kidney, were sampled with whole organs collected where possible. The samples were rinsed in saline, blotted dry, weighed, and then counted using a gamma counter (Cobra II; Packard Instruments, Meriden, CT). The energy windows used were 15–550 keV for ^{111}In and 150–600 keV for ^{225}Ac, which encompasses the chief ^{221}Fr and ^{213}Bi photopeaks. Samples of the injectates were used as decay correction standards. Data were expressed as % ID/g.

Therapy Studies. For the first therapy study, mice were randomized and placed into 6 treatment groups (n = 7–9). Groups consisted of growth control (no treatment) or i.p. administration of either native trastuzumab 2.5 μg, ^{225}Ac-labeled trastuzumab, 220 nCi or 110 nCi ×2 separated by 14 days, or ^{225}Ac-labeled HuM195, 220 nCi or 110 nCi ×2 separated by 14 days (specific activities were between 0.04 and 0.08 Ci/g).

In the second therapy study, mice were randomized and placed into 5 different treatment groups (n = 10). Groups consisted of growth control or i.p. administration of either ^{225}Ac-labeled trastuzumab, 225 nCi ×2 separated by 14 days or 110 nCi ×3 separated by 7 days, or ^{225}Ac-labeled HuM195, 225 nCi ×2 separated by 14 days or 110 nCi ×3 separated by 7 days. For both experiments treatment began 9 days after tumor implantation, and radiolabeled antibody concentrations were adjusted with native antibody to 2.5 μg/dose. In the second therapy experiment, the second administration to mice in the 110 nCi ×3 groups consisted of radioimmunoconjugate that was produced the preceding week. The radiochemical purity and immunoreactivity of the radioimmunoconjugates were unchanged after storage at 7 μCi/ml in 1% HSA at 4°C.

Mice were monitored daily and weighed twice weekly for evidence of treatment induced toxicity and disease progression. In this model, disease progression manifests as either extensive peritoneal ascites or severe weight loss.

Statistical Analysis. Survival curves were constructed using a Prism software package (Graphpad Software Inc., San Diego, CA) based on the method of Kaplan-Meier. Statistical comparisons among the different treatment groups were performed using the Mann-Whitney rank sum test. All tests were two-tailed with the level of statistical significance set at $P < 0.05$.

RESULTS

Radiolabeling and Quality Control. The radiochemical yields, radiochemical purities, and antigen binding activities of radioimmunoconjugates are summarized in Table 1. Greater than 99% of the radiometal is chelated by the DOTA derivative in the first step (data not shown), but the efficiency of the conjugation step is low, resulting in radiochemical yields of 7–17%. The radiochemical purities were good, at 93.8 ± 3.7%, but with low specific activities, 0.3–0.08 μCi/μg. Trastuzumab antigen binding activity was 72.0 ± 14.5%, but the variability between batches was large. This variance did not appear to be related to the different batches of antibody or the result of radiolysis, as the ^{111}In-labeled trastuzumab had as large a variability as the ^{225}Ac-labeled trastuzumab.

Internalization. Total cell-associated radioactivity increased over time of incubation reaching a 10-fold increase at 4 h (Fig. 2). The cell surface radioactivity increased 6-fold within the first 0.5 h and then remained constant. Internalized radioactivity increased 16-fold over 4 h and did not plateau. The constant membrane-bound activity implies that the HER-2/*neu* target receptor was being replaced at the cell membrane as the receptor was being internalized.

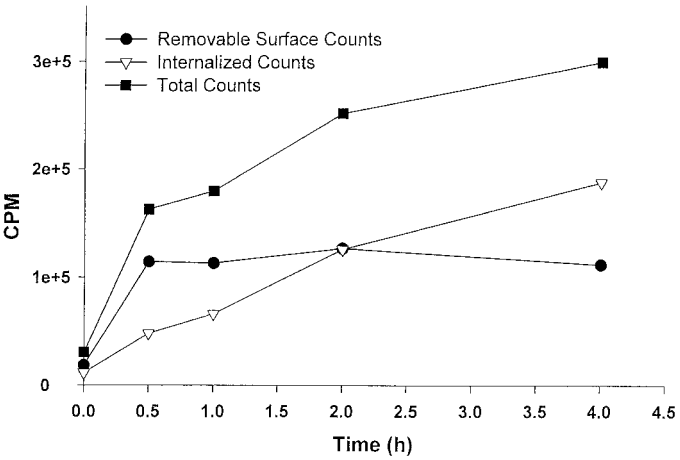

Fig. 2. Internalization time course of ^{225}Ac-labeled trastuzumab in SKOV3-NMP2 cells. ^{225}Ac-labeled trastuzumab, 10 ng/ml, was added to ice cold, blocked SKOV3-NMP2 cells, 10^7 cells/ml. Samples were removed and the cells transferred to a 37°C incubator where they were sampled at 0.5, 1, 2, and 4 h. Sampled cells were washed twice with ice-cold PBS and then an acidic stripping buffer [50 mM glycine/150 mM NaCl (pH 2.8)] was added. The cells were incubated for 10 min at room temperature and then centrifuged. The supernatants and cell pellets were transferred to scintillation vials for counting. The percentage of membrane bound (acid-strippable) and internalized counts were then determined.

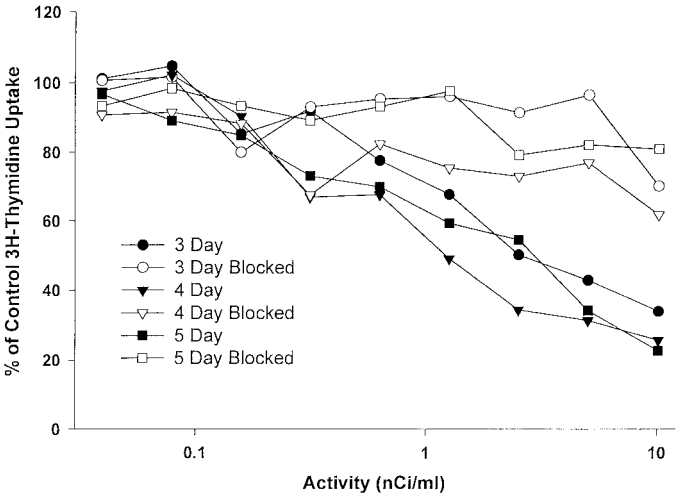

Fig. 3. Cell kill assay of ^{225}Ac-labeled trastuzumab in SKOV3-NMP2 cells. Serial dilutions of ^{225}Ac-labeled trastuzumab were added to SKOV3-NMP2 cells, 2.5×10^3 cells, in 96-well plates. Cell viability was determined by dividing the mean counts of the treated wells by the mean counts from control wells and multiplying by 100, n = 3. Half of the experiments were blocked with excess native trastuzumab. After 3, 4, or 5 days of incubation at 37°C, [^{3}H]thymidine was added and the plates were incubated overnight. The cells were collected and washed on filter paper and then counted in a scintillation counter. Data show means. Cell viability was determined by dividing the counts of the treated wells by the counts from control wells.

Table 1 *Summary of radiolabeling quality control results*

Radiochemical yield determined by dividing purified activity by the total activity applied to the chromatography column and then multiplying the result by 100. Radiochemical purity determined by instant TLC followed by analysis with a gas ionization detector. Binding activity determined by incubating 5 ng of radioimmunoconjugate with 10^7 SKOV3-NMP2 cells, then washing the cells with PBS, and collecting and counting the wash and cell pellet. Cell pellet cpm was then divided by the total cpm and multiplied by 100.

Radioimmunoconjugate	n	Radiochemical yield	Radiochemical purity	Antigen binding
^{225}Ac-trastuzumab	5	17.0 ± 6.8%	95 ± 2%	69 ± 14%
^{225}Ac-HuM195	4	11.1 ± 2.1%	92 ± 5%	N/A[a]
^{111}In-trastuzumab	3	10.4 ± 1.6%	94 ± 4%	76 ± 17%
^{111}In-HuM195	1	7%	99%	N/A

[a] N/A, not applicable.

Cell Cytotoxicity. The ^{225}Ac-labeled trastuzumab demonstrated specific cell killing with the ED_{50}, as measured by [^{3}H]thymidine uptake, being ~2.4 nCi/ml, 1.2 nCi/ml, and 2.8 nCi/ml after incubation, respectively, for 3, 4, and 5 days (Fig. 3). With a 10-day half-life only 19% of the ^{225}Ac would have decayed in 3 days, 24% in 4 days, and 29% in 5 days.

These ED_{50} values are an order of magnitude smaller than the values seen with other solid tumor cell lines (BT-474 and MCF7,

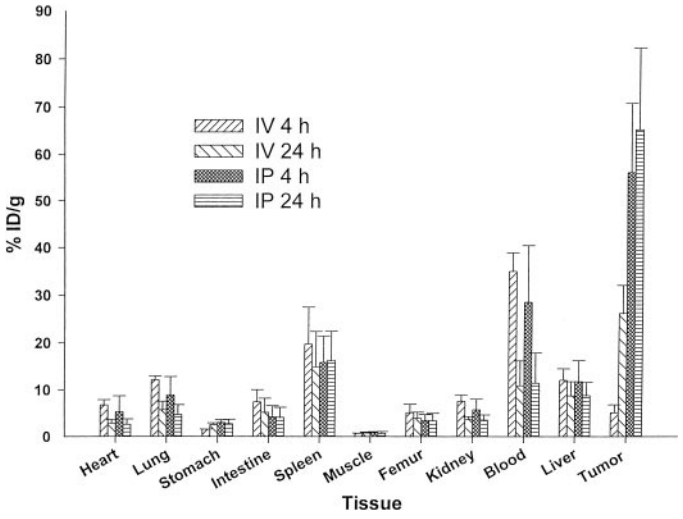

Fig. 4. Comparative biodistributions of i.p. and i.v. administered ^{111}In-labeled trastuzumab. Female athymic nude mice bearing 19-day-old i.p. xenografts of SKOV3-NMP2 cells were administered i.p. ^{111}In-labeled trastuzumab (n = 6–7) or i.v. ^{111}In-labeled trastuzumab (n = 4). Mice were sacrificed at 4 and 24 h after administration, and blood, tumor, heart, lung, stomach, intestine, spleen, muscle, bone, liver, and kidney were sampled, weighed, and then counted with a gamma counter. The % ID/g for each sample was then determined; *bars*, ±SE.

breast; NMB7, neuroblastoma; and LNCaP, prostate) and probably reflect an intrinsic radioresistance to α radiation. The SKOV3 cell line is radioresistant with respect to γ radiation, null for p53, and resistant to chemotherapeutic drugs (19).

Biodistribution of Antibody. Nineteen days after inoculation, tumor cells in mice formed distinct tumor nodules spread throughout the peritoneal cavity, with most nodules concentrated in the area around the spleen, stomach, pancreas, and the junction of the lobes of the liver. Removable tumor weight (mean of all of the mice sacrificed at 1- and 4-h time points) was 0.092 ± 0.025 g (n = 29).

i.p. administration of radioconstructs demonstrated high initial tumor uptake of ^{111}In-labeled trastuzumab, 56.0 ± 14.7% ID/g, at 4 h, which increased to 65.1 ± 17.1% ID/g at 24 h (Fig. 4). In contrast, i.v. administration demonstrated low initial tumor uptake (5.2 ± 1.7% ID/g at 4 h), which increased to 26.2 ± 5.9% ID/g at 24 h. The 11-fold higher initial tumor uptake after i.p. administration reflects ready accessibility of the radioimmunoconjugate to the periphery of tumor masses. The continued tumor uptake seen at the later time points probably indicated the added contribution from radioimmunoconjugate in blood. Normal organ values were similar at both time points with a slight elevation in most organs at 4 h after administration for the mice that received i.v. administration reflecting the higher initial blood activity. Normal organs with the highest uptake of radioimmunoconjugate were liver with 12.1 ± 2.5% ID/g for i.v. and 11.8 ± 0.7% ID/g for i.p. at 4 h, which decreased, respectively, to 8.7 ± 3.0% ID/g and 8.8 ± 2.8% ID/g at 24 h, and spleen with 19.7 ± 7.8% ID/g for i.v. and 15.8 ± 6.0% ID/g for i.p. at 4 h, which remained elevated at 14.9 ± 7.5% ID/g for i.v. and 16.2 ± 6.2% ID/g for i.p. at 24 h. These organ values probably reflect catabolism and uptake of radiometal rather than antibody targeting (20).

Comparison of i.p. Administration of ^{111}In-labeled Trastuzumab to ^{111}In-labeled HuM195 in Mice with i.p. SKOV3 Xenografts. The initial time points of 1 and 4 h show rapid tumor uptake of ^{111}In-labeled trastuzumab with 36.0 ± 11.4% ID/g at 1 h and 56.0 ± 14.7% ID/g at 4 h. Control ^{111}In-labeled HuM195 showed 13.0 ± 0.8% ID/g at 1 h and 18.6 ± 6.8% ID/g at 4 h (Fig. 5). The tumor uptake of ^{111}In-labeled HuM195 peaked at 4 h, which coincides with peak blood radioactivity, 27.8 ± 2.9% ID/g. Tumor and blood radioactivity of ^{111}In-labeled HuM195 declined at 24 h to 7.0 ± 3.9% ID/g and 12.3 ± 8.7% ID/g, respectively. In contrast, tumor uptake of ^{111}In-labeled trastuzumab continued to rise at 24 h, 65.08 ± 17.1, whereas blood radioactivity declined to 11.4 ± 6.4% ID/g. Peak normal organ radioactivity for both antibodies mirrored peak blood radioactivity with the spleen and liver the highest with 15.8 ± 5.6% ID/g and 11.8 ± 4.5% ID/g, respectively, for ^{111}In-labeled trastuzumab, and 9.7 ± 1.5% ID/g and 9.5 ± 2.1% ID/g, respectively, for ^{111}In-labeled HuM195.

Tumor radioactivity continued to increase through 48 h with ^{111}In-labeled trastuzumab, 71.4 ± 16.7% ID/g, whereas it decreased for ^{111}In-labeled HuM195 to 6.3 ± 1.2% ID/g. Blood radioactivity continued to decrease, and this drop was reflected in normal organs values.

Comparison of i.p. Administration of ^{111}In-labeled Trastuzumab to ^{225}Ac-labeled Trastuzumab in Mice with i.p. SKOV3 Xenografts. Tumor uptake and retention of ^{225}Ac- and ^{111}In-labeled trastuzumab was similar (Fig. 6). The major difference was lower peak blood radioactivity for the ^{225}Ac-labeled trastuzumab at 4 h and consequently lower normal organ uptake of radioactivity. The biodistribution studies demonstrate that ^{111}In is a useful surrogate for ^{225}Ac-labeled antibodies.

Therapy Studies. Tumor burden was estimated by sacrifice of 6 untreated control animals at the initiation of the therapy experiments. The tumor mass was 0.032 ± 0.004 g (n = 6) with tumor nodules recovered primarily around the spleen, stomach, and pancreas.

Toxicity, as defined as a >10% weight loss, was not observed in the first therapy experiment. Additionally, there were no early, treatment-related deaths.

The median survival times for growth control mice and mice treated with a single dose of 2.5 μg of native trastuzumab were 33 and 37 days, respectively, after inoculation of tumor cells (Fig. 7). The difference between these two groups was not statistically significant. Mice treated with 220 nCi of ^{225}Ac-labeled trastuzumab and those

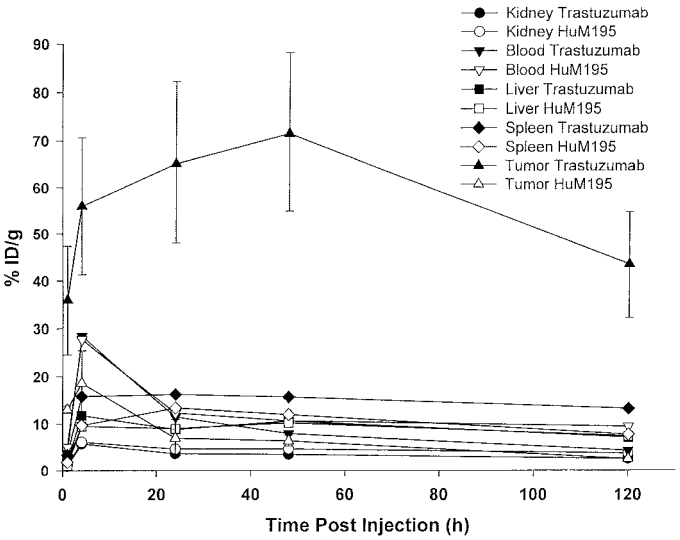

Fig. 5. Comparative biodistributions of i.p. administered ^{111}In-labeled trastuzumab and ^{111}In-labeled HuM195. Female athymic nude mice bearing 19-day-old i.p. xenografts of SKOV3-NMP2 cells were administered i.p. ^{111}In-labeled trastuzumab (n = 6–7) or ^{111}In-labeled HuM195 (n = 3–4). Mice were sacrificed at 1, 4, 24, 48, and 120 h after administration, and blood, tumor, heart, lung, stomach, intestine, spleen, muscle, bone, liver, and kidney were sampled, weighed, and then counted with a gamma counter. The % ID/g for each sample was then determined; *bars*, ± SE. For clarity, values for heart, lung, stomach, intestine, muscle, and femur are not shown. These tissues have <5% ID/g for all time points with the exception of lung (8.9% ID/g at 4 h for ^{111}In-labeled trastuzumab and 8.6% ID/g, 5.6% ID/g, and 5.7% ID/g at 4, 24, and 48 h for ^{111}In-labeled HuM195).

treated with 220 nCi or 110 nCi ×2 ^{225}Ac-labeled HuM195, fractions separated by 14 days, had median survival times of 52, 50, and 50 days, respectively, after inoculation of tumor cells. The difference between groups was not statistically significant. The difference between these groups and the mice that received either no treatment or native trastuzumab was statistically significant ($P = 0.0002$). Mice that received 110 nCi ×2 of ^{225}Ac-labeled trastuzumab fractions separated by 14 days had a median survival time of 65 days, which was statistically significant when compared against all of the other treatment groups except mice that received 200 nCi of ^{225}Ac-labeled trastuzumab ($P = 0.297$).

In the second therapy experiment, 10–12% weight loss was observed 1 day after the third administration of 110 nCi and the second administration of 225 nCi, respectively, of ^{225}Ac-labeled HuM195. These groups did not recover their weight before succumbing to disease progression or treatment-related death. Mice that received 110 nCi ×3 of ^{225}Ac-labeled trastuzumab experienced 10% weight loss after the first and third administration, but recovered to pretreatment weight within 2 weeks of their last administration. Mice that received 225 nCi ×2 of ^{225}Ac-labeled trastuzumab never lost >6% of their pretreatment weight.

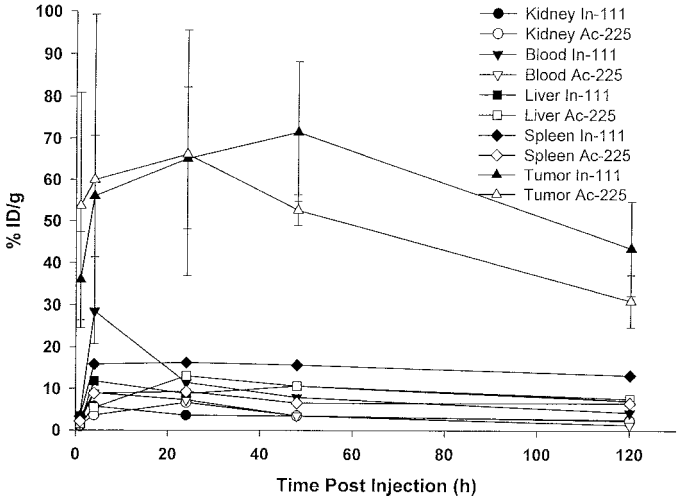

Fig. 6. Comparative biodistributions of i.p. administered ^{225}Ac- and ^{111}In-labeled trastuzumab. Female athymic nude mice bearing 19-day-old i.p. xenografts of SKOV3-NMP2 cells were administered i.p. ^{225}Ac-labeled trastuzumab ($n = 5$) or ^{111}In-labeled trastuzumab ($n = 6–7$). Mice were sacrificed at 1, 4, 24, 48, and 120 h after administration, and blood, tumor, heart, lung, stomach, intestine, spleen, muscle, bone, liver, and kidney were sampled, weighed, and then counted with a gamma counter. The % ID/g for each sample was then determined. For clarity, values for heart, lung, stomach, intestine, muscle, and femur are not shown. These tissues have <5% ID/g for all time points with the exception of lung (^{111}In-labeled trastuzumab, 8.9% ID/g at 4 h); *bars*, ±SE.

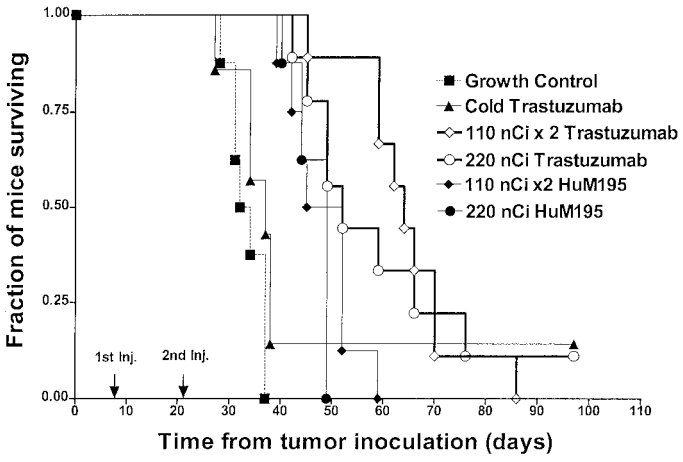

Fig. 7. Kaplan-Meier plot showing survival of mice bearing i.p. SKOV3-NMP2 xenografts. In this therapy experiment, treatment of mice (groups $n = 7–9$) was given 9 and 23 days after tumor inoculation with i.p.-administered antibody or radioimmunoconjugate. Treatment times marked by *arrows* on plot. Mice were monitored for signs of morbidity, at which time they were sacrificed.

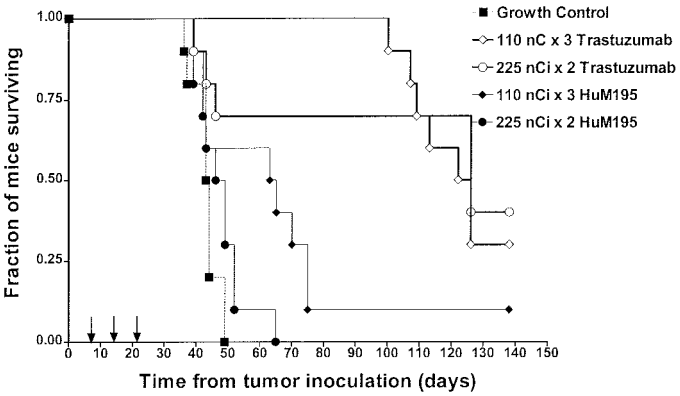

Fig. 8. Kaplan-Meier plot showing survival of mice bearing i.p. SKOV3-NMP2 xenografts. In this therapy experiment, mice (groups $n = 10$) were treated 9, 16, and 23 days after tumor inoculation with i.p.-administered radioimmunoconjugate. Mice were monitored for signs of morbidity, at which time they were sacrificed.

Petechia appeared in mice 11–15 days after the last administration of radioimmunoconjugate. The frequency was 2 of 10 mice treated with 110 nCi ×3 of ^{225}Ac-labeled HuM195, 2 of 10 mice treated with 225 nCi ×2 of ^{225}Ac-labeled HuM195, and 3 of 10 mice treated with 225 nCi ×2 of ^{225}Ac-labeled trastuzumab. All of the mice died within 4–8 days of the appearance of petechia.

Two additional mice in each of the 110 nCi ×3 and 225 nCi ×2 ^{225}Ac-labeled HuM195 groups presented with anemia caused by massive, bloody ascites. Necropsy of sacrificed mice demonstrated the occurrence of tumor in all of the mice. Bloody ascites is an end point for this tumor model, but it is possible that the loss of platelets may have accelerated the appearance of ascites.

The median survival time for growth control mice was 44 days (Fig. 8). Mice that received ^{225}Ac-labeled HuM195, 225 nCi ×2 separated by 14 days had a medium survival of 48 days. The difference in median survival between these groups was not significant. Mice that received ^{225}Ac-labeled HuM195, 110 nCi ×3 separated by 7 days had a median survival of 64 days. The difference in median survival between this group and growth control was significant, $P = 0.033$, as was the difference between this group and the mice that received ^{225}Ac-labeled HuM195, 225 nCi ×2 ($P = 0.049$).

Mice that received ^{225}Ac-labeled trastuzumab,110 nCi ×3, separated by 7 days had a median survival time of 124 days. Mice that received ^{225}Ac-labeled trastuzumab, 225 nCi ×2 separated by 14 days had an overall median survival time of 126 days. However, 3 mice in this treatment group died early with anemia, petechiae, or bleeding, suggesting bone marrow failure. The median survival times for the ^{225}Ac-labeled trastuzumab treatment groups were significantly different from all of the other treatment groups ($P \leq 0.043$), but they were not significantly different between themselves.

The first therapy study demonstrates a survival advantage for mice that received i.p.-administered ^{225}Ac-labeled HuM195. This advantage from nonspecific irradiation by the radioimmunoconjugate is abrogated in the second therapy study by the increased toxicity incurred from the increased accumulative administered activity and decreased time interval between fractions. The ^{225}Ac-labeled trastuzumab continued to demonstrate a survival advantage in the second therapy study, but toxicity was evident at the 225 nCi ×2 activity level.

DISCUSSION

For RIT of micrometastatic disease α particle emitters have several advantages over β emitters. Unlike β emitters, α emitters do not rely on a radiation field effect for cytotoxicity. Their high linear energy transfer, 80–100 keV/μm, compared with 0.2 keV/μm for β emitters, allows isolated single cells to be killed by the radioimmunoconjugate targeted to those cells. α particle path lengths are also roughly the same dimension as small clusters of target cells. A higher percentage of the energy of the decays will be deposited within these clusters than can be achieved with β particle emitters, reducing damage to the surrounding normal tissue. Additionally, preclinical and clinical results support higher relative biological effect (RBE) values for α emitters and, therefore, suggest that an enhanced therapeutic ratio may exist with α emitters (21–24). Furthermore, unlike β emitters, the clustered, double-strand DNA breaks induced by α emitters are independent of the dose rate, which decreases exponentially as radioisotopes decay (25).

These experiments demonstrated the efficacy of regional RIT with an internalizing antibody coupled to a ^{225}Ac *in vivo* generator in a model of ovarian peritoneal carcinomatosis. With the appropriate dosing schedule, prolonged survival was achieved without apparent gross toxicity in a model of advanced chemotherapy and radiation-resistant disease.

The two-step labeling methodology produces radioimmunoconjugates with suitable radiochemical purity and immunoreactivity. The radiochemical yields were low but sufficient for preclinical and clinical trials, as the extreme potency of these reagents allows studies to commence with 50–200 nCi activity. Human doses would be expected to be in the 10–100 μCi range. One shortcoming to this radiolabeling methodology is the low specific activity of the radioimmunoconjugates, wherein only one antibody of ~1000 is radiolabeled. This may preclude the use of these reagents in diseases with relatively low antigen expression.

The tumor uptake is quite high in this model and exceeds that of other published i.p. xenograft/i.p. administration models (26–29). The high uptake may result from the high expression and internalization rate of the HER-2/*neu* antigen and also the large surface area that results from having many small tumor nodules. Larger nodules are known in preclinical (26) and in clinical studies (30) to have lower uptake of activity, which may relate to a smaller surface area to volume ratio. The tumor and normal organ biodistribution of ^{225}Ac-labeled trastuzumab was similar to ^{111}In-labeled trastuzumab and suggests that ^{111}In-labeled antibodies can serve as surrogates for determining the pharmacokinetics and biodistribution of ^{225}Ac-labeled antibodies. This allows dosimetric calculations to be performed on data from previous animal models and clinical trials with ^{111}In-labeled antibody studies. However, as discussed below, the biodistribution of some ^{225}Ac daughters may not be modeled by ^{111}In-labeled antibodies.

The first therapy study suggests that fractionated therapy with ^{225}Ac-labeled trastuzumab may be more effective than a single administration of ^{225}Ac-labeled trastuzumab. The median survival is longer with fractionated therapy, but the two populations are not distinct. In the second therapy study using two different fractionation activities and schedules, the smaller, more frequent activity, 110 nCi ×3, weekly, had an equivalent median survival as 225 nCi ×2 administered 14 days apart. More importantly, the 110 nCi ×3 schedule was without the early mortality seen with the higher activity.

Repeat administration may be necessary to treat large clusters of tumor cells, as spheroid studies demonstrate that the distribution of radioimmunoconjugates is restricted to the outer cell layers (31). An adequate time interval may be required to clear dead cells and expose viable cells underneath. Fortunately, the required number of fractions may be low, as spheroids up to 20–30 cells in diameter can be killed by the small radiation field effect generated by α particle emitting radioimmunoconjugates (31).

An internalizing antibody was used in these studies to increase cytotoxicity toward targeted cells. α particles originating on the cell surface have an estimated 30% probability of traversing a cell (1). Internalizing antibodies increase this likelihood of decays traversing the cell and the probability of hitting the nucleus. Internalization rate can be increased through two modifications of antibody structure, dimerization and cationization. Dimerization increases avidity thereby decreasing the dissociation rate, resulting in higher cell membrane antibody concentration (32). Internalization rates increased 2–4-fold through clustering of antigen or Fc receptors (32, 33). For i.p. administration, dimerization is of particular interest, as the larger size of the radioimmunoconjugate should slow the egress of the drug from the peritoneal cavity. Cationization increases the isoelectric point of an antibody, and can markedly increase binding and internalization rates through absorptive-mediated endocytosis (34).

Internalizing antibodies may be crucial for the use of ^{225}Ac, as the first radioactive daughter, francium-221 (^{221}Fr) is not bound by the chelate after the change in periodicity and the nuclear recoil that accompanies the α particle emission. Whereas the prospect of unbound radiometals is worrisome, our data suggests that ^{225}Ac daughters are sequestered inside cells after internalization of ^{225}Ac-labeled antibodies and that ^{225}Ac daughters from untargeted radioimmunoconjugate may not represent an insurmountable problem (4).[4]

As opposed to mice where peak blood radioactivity is seen at 4 h, clinical studies demonstrate that i.p. administration results in the slow release of radioactivity into the blood with peak serum radioactivity occurring ~2 days after administration, representing 13–30% of the total administered activity (10, 13). With rhenium-186, i.p. administration can increase the maximum tolerated dose by 2/3 over i.v. administration (10). Rhenium-186 has a 3.7-day half-life, so by 48 h 31% of the radioisotope has decayed. In contrast, with ^{225}Ac only 13% of the radioisotope would have decayed. However, the longer half-life of Ac-225 may result in greater biological clearance, particularly of chelated Ac-225 before appreciable decay occurs.

Trastuzumab and the SKOV3 animal model were selected for proof of principle of regional therapy with an ^{225}Ac *in vivo* generator because of the aggressive growth, high antigen expression, and high degree of internalization of the antibody/antigen complex of the target cells. However, for clinical development, other antibodies may be more appropriate as the incidence of HER-2/*neu* overexpression in ovarian cancer is relatively low, 25–30% (35, 36). A more appropriate target may be the internalizing, high affinity folate receptor, overexpressed in ~90% of nonmucinous epithelial ovarian tumors (37). Moreover, these data suggests a possibility of treating other cancers with i.p. carcinomatosis, such as colon cancer.

In summary, we have tested the use of internalizing *in vivo* α particle generators in a regional model of advanced ovarian cancer. Long-term survival was achieved. The results suggest that i.p. RIT with ^{225}Ac is feasible for the treatment of micrometastatic disease and that additional development of this modality is warranted.

REFERENCES

1. Nikula, T. K., McDevitt, M. R., Finn, R. D., Wu, C., Kozak, R. W., Garmestani, K., Brechbiel, M. W., Curcio, M. J., Pippin, C. G., Tiffany-Jones, L., Geerlings M. W. Sr., Apostolidis, C., Molinet, R., Geerlings, M. W., Jr., Gansow, O. A., and Scheinberg, D. A. α-Emitting bismuth cyclohexylbenzyl DTPA constructs of recombinant

[4] P. E. Borchardt, M. Meiderer, M. R. McDevitt, and D. A. Scheinberg, unpublished observations.

humanized anti-CD33 antibodies: pharmacokinetics, bioactivity, toxicity and chemistry. J. Nucl. Med., *40:* 166–176, 1999.
2. Sgouros, G., Ballangrud, A. M., Jurcic, J. G., McDevitt, M. R., Humm, J. L., Erdi, Y. E., Mehta, B. M., Finn, R. D., Larson, S. M., and Scheinberg, D. A. Pharmacokinetics and dosimetry of an α-particle emitter labeled antibody: ^{213}Bi- HuM195 (anti-CD33) in patients with leukemia. J. Nucl. Med., *40:* 1935–1946, 1999.
3. McDevitt, M. R., Sgouros, G., Finn, R. D., Humm, J. L., Jurcic, J. G., Larson, S. M., and Scheinberg, D. A. Radioimmunotherapy with α-emitting nuclides. Eur. J. Nucl. Med., *25:* 1341–1351, 1998.
4. McDevitt, M. R., Ma, D., Lai, L. T., Simon, J., Borchardt, P. E., Frank, R. K., Wu, K., Pellegrini, V., Curcio, M. J., Miederer, M., Bander, N. H., and Scheinberg, D. A. Tumor therapy with targeted atomic nanogenerators. Science (Wash. DC), *294:* 1537–1540, 2001.
5. McDevitt, M. R., Finn, R. D., Sgouros, G., Ma, D., and Scheinberg, D. A. An ^{225}Ac/^{213}Bi generator system for therapeutic clinical applications: construction and operation. Appl. Radiat. Isot., *50:* 895–904, 1999.
6. McGuire, W. P. Primary treatment of epithelial ovarian malignancies. Cancer (Phila.), *71*(Suppl.)*:* 1541–1550, 1993.
7. Bolis, G., Villa, A., Guarnerio, P., Ferraris, C., Gavoni, N., Giardina, G., Melpignano, M., Scarfone, G., Zanaboni, F., and Parazzini, F. Survival of women with advanced ovarian cancer and complete pathological response at second-look laparotomy. Cancer (Phila.), *77:* 128–131, 1996.
8. Epenetos, A. A., Munro, A. J., Stewart, S., Rampling, R., Lambert, H. E., McKenzie, C. G., Soutter, P., Rahemtulla, A., Hooker, G., and Sivolapenko, G. B. Antibody-guided irradiation of advanced ovarian cancer with intraperitoneally administered radiolabeled monoclonal antibodies. J. Clin. Oncol., *5:* 1890–1899, 1987.
9. Crippa, F., Bolis, G., Seregni, E., Gavoni, N., Scarfone, G., Ferraris, C., Buraggi, G. L., and Bombardieri, E. Single–dose intraperitoneal radioimmunotherapy with the murine monoclonal antibody I-131-Mov18: clinical results in patients with minimal disease of ovarian cancer. Eur. J. Cancer, *31:* 686–690, 1995.
10. Breitz, H. B., Durham, J. S., Fisher, D. R., and Weiden, P. L. Radiation-absorbed dose estimates to normal organs following intraperitoneal ^{186}Re- labeled monoclonal antibody: methods and results. Cancer Res., *55*(Suppl.)*:* 5817s–5822s, 1995.
11. Nicholson, S., Gooden, C. S., Hird, V., Maraveyas, A., Mason, P., Lambert, H. E., Meares, C. F., and Epenetos, A. A. Radioimmunotherapy after chemotherapy compared to chemotherapy alone in the treatment of advanced ovarian cancer: a matched analysis. Oncol. Rep., *5:* 223–226, 1998.
12. Buijs, W. C. A. M., Tibben, J. G., Boerman, O. C., Molthoff, C. F. M., Massuger, L. F. A. G., Koenders, E. B., Schijf, C. P. T., Siegel, J. A., and Corstens, F. H. M. Dosimetric analysis of chimeric monoclonal antibody cMOv18 IgG in ovarian carcinoma patients after intraperitoneal and intravenous administration. Eur. J. Nucl. Med., *25:* 1552–1561, 1998.
13. Meredith, R. F., Partridge, E. E., Alvarez, R. D., Khazaeli, M. B., Plott, G., Russell, C. D., Wheeler, R. H., Liu, T., Grizzle, W. E., Schlom, J., and LoBuglio, A. F. Intraperitoneal radioimmunotherapy of ovarian cancer with lutetium-177-CC49. J. Nucl. Med., *37:* 1491–1496, 1996.
14. Carter, P., Presta, L., Gorman, C. M., Ridgeway, J. B. B., Henner, D., Wong, W. L. T., Rowland, A. M., Kotts, C., Carver, M. E., and Shepard, H. M. Humanization of an anti-p185^{HER2} antibody for human cancer therapy. Proc. Natl. Acad. Sci. USA, *89:* 4285–4289, 1992.
15. Co, M. S., Avdalovic, N. M., Caron, P. C., Avdalovic, M. V., Scheinberg, D. A., and Queen, C. Chimeric and humanized antibodies with specificity for the CD33 antigen. J. Immunol., *148:* 1149–1154, 1991.
16. Mujoo, K., Maneval, D. C., Anderson, S. C., and Gutterman, J. U. Adenoviral-mediated p53 tumor suppressor gene therapy of human ovarian carcinoma. Oncogene, *12:* 1617–1623, 1996.
17. McDevitt, M. R., Ma, D., Simon, J., Frank, R. K., Kiefer, G. E., and Scheinberg, D. A. Design and synthesis of Actinium-225 Radioimmunopharmaceuticals. Appl. Radiat. Isot., *57:* 841–847, 2002.
18. Nikula, T. K., Curcio, M. J., Brechbiel, M. W., Gansow, O. A., Finn, R. D., and Scheinberg, D. A. A rapid single vessel method for preparation of clinical grade ligand conjugated monoclonal antibodies. Nucl. Med. Biol., *22:* 387–390, 1995.
19. Concin, N., Zeillinger, C., Stimpfel, M., Schiebel, I., Tong, D., Wolff, U., Reiner, A., Leodolter, S., and Zeillinger, R. p53-dependent radioresistance in ovarian cancer cell lines. Cancer Lett., *150:* 191–199, 2000.
20. Scheinberg, D. A., and Strand, M. Kinetic and catabolic considerations of monoclonal antibody targeting in erythroleukemic mice. Cancer Res., *43:* 265–272, 1983.
21. Behr, T. M., Behe, M., Stabin, M. G., Wehrmann, E., Apostolidis, C., Molinet, R., Strutz, F., Fayyazi, A., Wieland, E., Gratz, S., Koch, L., Goldenberg, D. M., and Becker, W. High-linear energy transfer (LET) α verse low-LET β emitters in radioimmunotherapy of solid tumors: therapeutic efficacy and dose-limiting toxicity of ^{213}Bi- versus ^{90}Y-labeled CO17-1A Fab' fragments in a human colonic cancer model. Cancer Res., *59:* 2635–2643, 1999.
22. Behr, T. M., Sgouros, G., Stabin, M. G., Behe, M., Angerstein, C., Blumenthal, R. D., Apostolidis, C., Molinet, R., Sharkey, R. M., Koch, L., Goldenberg, D. M., and Becker, W. Studies on the red marrow dosimetry in radioimmunotherapy: an experimental investigation of factors influencing the radiation-induced myelotoxicity in therapy with β-, Auger/conversion electron-, or α-emitters. Clin. Cancer Res., *5:* 3031s–3043s, 1999.
23. Sgouros, G., Ballangrud, A. M., Hamacher, K. A., Jurcic, J. G., Panageas, K. S., McDevitt, M. R., Finn, R. D., Larson, S. M., and Scheinberg, D. A. β- vs. α-emitter dose-response analysis in patients. J. Nucl. Med., *41*(Suppl.)*:* 82P, 2000.
24. Pouget, J. P., and Mather, S. J. General aspects of the cellular response to low- and high-LET radiation. Eur. J. Nucl. Med., *28:* 541–561, 2001.
25. Wilbur, D. S. Potential use of α emitting radionuclides in the treatment of cancer. Antibody Immunoconjug. Radiopharm., *4:* 85–97, 1991.
26. Ward, B. G., and Wallace, K. Localization of monoclonal antibody HMFG2 after intravenous and intraperitoneal injection into nude mice bearing subcutaneous and intraperitoneal human ovarian cancer xenografts. Cancer Res., *47:* 4714–4718, 1987.
27. Rowlinson, G., Snook, D., Busza, A., and Epenetos, A. A. Antibody-guided localization of intraperitoneal tumors following intraperitoneal or intravenous administration. Cancer Res., *47:* 6528–6531, 1987.
28. Andersson, H., Lindegren, S., Back, T., Jacobsson, L., Leser, G., and Horvath, G. The curative and palliative potential of the monoclonal antibody Mov18 labeled with ^{211}At in nude mice with intraperitoneally growing ovarian cancer xenografts. Acta Oncol., *39:* 741–745, 2000.
29. Gadina, M., Canevari, S., Ripamonti, M., Mariani, M., and Colnaghi, M. I. Preclinical pharmacokinetics and localization studies of the radioiodinated anti- ovarian carcinoma MAb MOv18. Nucl. Med. Biol., *18:* 403–408, 1991.
30. Chatal, J. F., Saccavini, J. C., Gestin, J. F., Thedrez, P., Curtet, C., Kremer, M., Guerreau, D., Nolibe, D., Fumoleau, P., and Gulliard, Y. Biodistribution of indium-111-labeled OC 125 monoclonal antibody intraperitoneally injected into patients operated on for ovarian cancer. Cancer Res., *49:* 3087–3094, 1989.
31. Kennel, S. J., Stabin, M., Roeske, J. C., Foote, L. J., Lankford, P. K., Terzaghi- Howe, M., Patterson, H., Barkenbus, J., Popp, D. M., and Mirzadeh, S. Radiotoxicity of bismuth-213 bound to membranes of monolayer and spheroid cultures of tumor cells. Radiat. Res., *151:* 244–256, 1999.
32. Wolff, E. A., Schreiber, G. J., Cosand, W. L., and Raff, H. V. Monoclonal antibody homodimers: enhanced antitumor activity in nude mice. Cancer Res., *53:* 2560–2565, 1993.
33. Caron, P. C., Laird, W., Co, M. S., Avdalovic, N. M., Queen, C., and Scheinberg, D. A. Engineered humanized dimeric forms of IgG are more effective antibodies. J. Exp. Med., *176:* 1191–1195, 1992.
34. Pardridge, W. M., Bickel, U., Buciak, J., Yang, J., Diagne, A., and Aepinus, C. Cationization of a monoclonal antibody to the human immunodeficiency virus REV protein enhances cellular uptake but does not impair antigen binding of the antibody. Immunol. Lett., *42:* 191–195, 1994.
35. Berchuck, A., Kamel, A., Whitaker, R., Kerns, B., Olt, G., Kinney, R., Soper, J. T., Dodge, R., Clarke-Pearson, D. L., Marks, P., McKenzie, S., Yin, S., and Bast, R. C., Jr. Overexpression of HER-2/neu is associated with poor survival in advanced epithelial ovarian cancer. Cancer Res., *50:* 4087–4091, 1990.
36. Rubin, S. C., Finstad, C. L., Wong, G. Y., Almadrones, L., Plante, M., and Lloyd, K. O. Prognostic significance of HER-2/neu expression in advanced epithelial ovarian cancer: a multivariate analysis. Am. J. Obstet. Gynecol., *168:* 162–169, 1993.
37. Miotti, S., Canevari, S., Menard, S., Mezzanzanica, D., Porro, G., Pupa, S. M., Regazzoni, M., Tagliabue, E., and Colnaghi, M. I. Characterization of human ovarian carcinoma-associated antigens defined by novel monoclonal antibodies with tumor-restricted specificity. Int. J. Cancer, *39:* 297–303, 1987.